



A Closed Loop Control of Power Factor Correction AC-DC Power Supply with ZVS

Harisha Valluri and Bezawada Eedukondalu

Department of Electrical and Electronics Engineering, NRI Institute of Technology, Agiripalli, India.
Corresponding Author Mail Id: harishavalluri217@gmail.com

To Cite this Article

Harisha Valluri and Bezawada Eedukondalu. A Closed Loop Control of Power Factor Correction AC-DC Power Supply with ZVS. *International Journal for Modern Trends in Science and Technology* 2022, 8 pp. 55-61.
<https://doi.org/10.46501/IJMTST0801010>

Article Info

Received: 24 November 2021; Accepted: 31 December 2021; Published: 04 January 2022

ABSTRACT

The use of electronic equipment is increasing in the modern world Therefore, it is mandatory to ensure that any electronic that is connected to the ac supply is tested for harmonic content. This is done by using the sinusoidal current circuit with phase shift (the Power Factor Correction [PFC]) There are numerous ways to produce a sinusoidal line This paper describes a leaky power supply that provides a boost inductor function with an isolated from the transformer' In the isolated power supply, the bulk capacitor is utilised for limiting of the start surge voltage. A switch controller developed for voltage regulation and input power factor control is created.

Keywords— AC–DC power conversion, power factor correction, transformer leakage inductance.

1. INTRODUCTION

Many computers and other electronic equipment are required to use a power factor-correction (PFC) unit (PSU) due to the increasing use of single-phase electrical connections. the current drawn from the line (from the line source) is of lowest-order harmonic free (HT) a wide literature on power factor correction has been produced, and numerous power factor correction methods employ high-frequency switching

In order to get the voltage shape required for low THD and high PF, use input current must be regulated. For many uses, the power supply must provide a regulated dc voltage. A fundamental part of all-of-the-the-the-architecture boosting or step-up architectures is the inductor that gives rise to adjustable current input. The flyback converter can be derived

from the boost converter, but with an isolation transformer [5] used.

Lower power levels traditionally had to be accommodated by flyback transformers For higher levels of power (≥ 500 W), separate dc to dc voltage regulator with boost converter is required.

2. PROPOSED PFC ARCHITECTURE

The leakage inductance is used as the booster induct in this PFC design. Leak minimization is usually done on most DC converters, but in the case of resonant and soft-switching architectures, lowering the inductance is beneficial due to electrical losses.

This paper suggests using a controlled leakage inductance to achieve both power factor correction and galvanic isolation with a single magnetic unit.

Using a soft initialization technique, the large bulk capacitor is taken to a high charge when the device is turned on. used for bi-directional excitation, with the energy contained in the leakage inductance The listed architecture is a good option for a voltage-level flyback converter.

The method is suitable for wide-gamut devices. In standard vehicle applications, LED lighting, onboard electronics, and an onboard charger are popular.

PROPOSED ARCHITECTURE

Figure 3.1 illustrates a schematic diagram. Until being applied to a transformer TX, a traditional four-diode full-wave rectifying voltage supply generates VR. The half-bridge is made up of two switches, M1 and M2, that are both worked at 50% duty cycle at the switching frequency and a capacitor (C1, C2) that is split in half.

S2 prevents voltage from increasing above the saturation in the transformer's primary. The values of C1 and C2 are such that at the mains frequency f and a low power level, the reactor follower's excitation voltage follows the mains. Though they are sufficiently large fixed voltage sources, their values don't cause transform and load inductances to resonate. see Fig. 2 The rms voltage of the mains is $V_M = 2V_{AC}$. amplitude of the primary voltage $V_P(t)$ is switched (mid-mid-speed mid-amplitude).

The transformer symbol in Figure 1 is drawn so that the use of leakage inductance is emphasised. To operate the device, use the [Figure 1] bistable circuit shown in figure 1

3.THEORY OF OPERATION

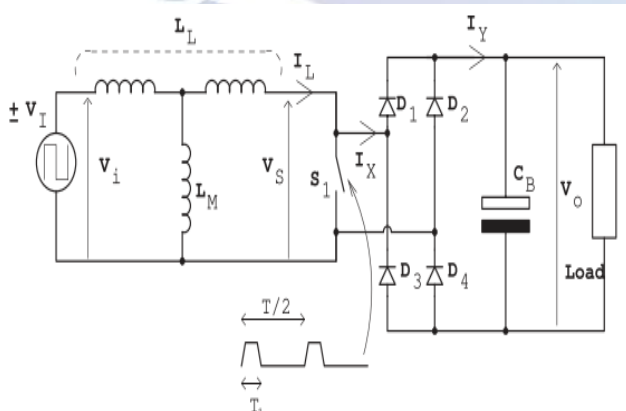


Fig.1 .Simplified circuit model for the proposed power supply.

The proposed powersymp is represented here as a basic circuit model. The transformer is equal to a 50 percent

square wave with an if the converter's input frequency is high in contrast to the ac frequency. The secondary is related to the transformer model shown in Figure 3.2.

$$V_I[kT] = \left| V_P(kT) \frac{N_s}{N_p} \right| \quad (2.1)$$

The circuit operates on the theory that transformer magnetising inductance has little effect on the operation other than to increase the source's magnetising current simulations show that using a factor of 5 less than the actual magnetising current, have little impact on the overall circuit behaviour The total transformer leakage inductance is denoted L_L and the current out of the secondary winding is denoted $I(t)$.

The operation is that of a step-up converter, as seen in Fig. 3. In the beginning of a switching cycle, the input voltage shifts to $[V_I]$ and the S1 switching is turned on. The current (flow) increases linearly while the leakage inductance leak. When the S1 switch is turned OFF, the current in the leaky bridge formed by D1, D2, D3, and D4 flows through the CB to the system load. After a period of negative change, the input voltage remains constant, but the inductor current's sign changes Two distinct operating modes are determined by whether the circuit's leakage current starts with zero and returns to zero before time T_2 , called discontinuous conduction (DC), or is discontinuous until time T_2 and then has a positive (P) for a brief period of time afterward, which is called non-continuous conduction (CCM).

to increase circuit power factor, the circuit is operated to conform to the input Timing periods are now covered in detail to explain the input current drawn

Discontinuous Conduction Mode

Figshows the input voltage V_{ti} and the secondary voltage V_t as well as the leak current I_L , with current out of the DCM for the associated." The leakage current $I_L(t)$ rises from zero to $+I_P$ after time T_1

$$I_P = V_I T_1 / L_L. \quad (3.2)$$

When the shorting switch S1 opens, the inductor current fallback to zero over a period T_2 with the relationship

$$I_P = (V_O - V_I) T_2 / L_L. \quad (3.3)$$

The sum of the periods must be less than the half period $T/2$ to ensure operation in the DCM or

$$T_1 + T_2 \leq \frac{T}{2}. \quad (3.4)$$

The average input current to the transformer model (ignoring the magnetizing inductance) over the period $T/2$ can then be calculated as follows:

$$I_L^* = \frac{1}{2} I_P \frac{T_1 + T_2}{\frac{T}{2}} \quad (3.5)$$

And combining with (2) and (3), the average input current is

$$I_L^* = \frac{T_1^2}{T L_L} \left(\frac{V_I V_O}{V_O - V_I} \right). \quad (3.6)$$

The actual input current from the ac source is a scaled version of this current and is

$$I_M = \frac{1}{2} \frac{N_s}{N_p} I_L^* \quad (3.7)$$

With any contribution from the magnetizing inductance averaging to zero over each T period.

It is apparent by considering (1) and (7), that achieving unity power factor in the input source is equivalent to controlling the current value I^*L to be directly proportional to V_I . Denoting the constant of proportionality as G_M , or $I_L^* = G_M V_I$, then substituting in (6) and rearranging yields the equation

$$T_1 = \sqrt{G_M T L_L \left(\frac{V_O - V_I}{V_O} \right)}. \quad (3.8)$$

The equation shows that given a constant of proportionality as G_M , the required time period T_1 can be calculated by knowledge of the system parameters L_L and T , measurement of the output voltage V_O and calculating V_I by measurement of the rectified input source voltage and scaling by a factor of $1/2 N_s/N_p$

Continuous Conduction Mode

Fig. 3.3(b) shows the input voltage $V_i(t)$, the secondary voltage $V_s(t)$, the leakage inductor current $I_L(t)$, and the current into and out of the output rectifier $I_X(t)$ and $I_Y(t)$ as well as the switch current $I_{S1}(t)$, for the circuit operating in CCM. With the shorting switch $S1$ closed, the leakage inductor current $I_L(t)$ rises from the value $-IE$ to the value $+IP$ over the set period T_1 , thus

$$I_P + I_E = V_I T_1 / L_L. \quad (3.9)$$

When the shorting switch $S1$ opens, the inductor current falls back to $+IE$ over a period $T_2 = T/2 - T_1$ with the relationship

$$I_P - I_E = (V_O - V_I) T_2 / L_L. \quad (3.10)$$

The average input current to the transformer model (ignoring the magnetizing inductance) over the period $T/2$ can then be calculated as follows:

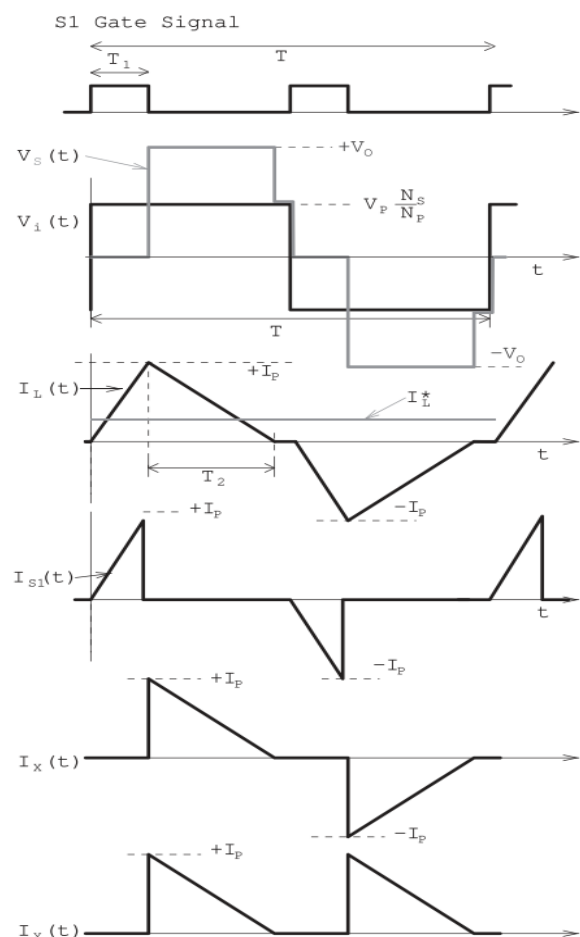
$$I_L^* = \frac{\frac{1}{2}(I_P - I_E)T_1 + \frac{1}{2}(I_P + I_E)T_2}{\frac{T}{2}} \quad (3.11)$$

And combining with (9) and (10), the average input current can be shown as

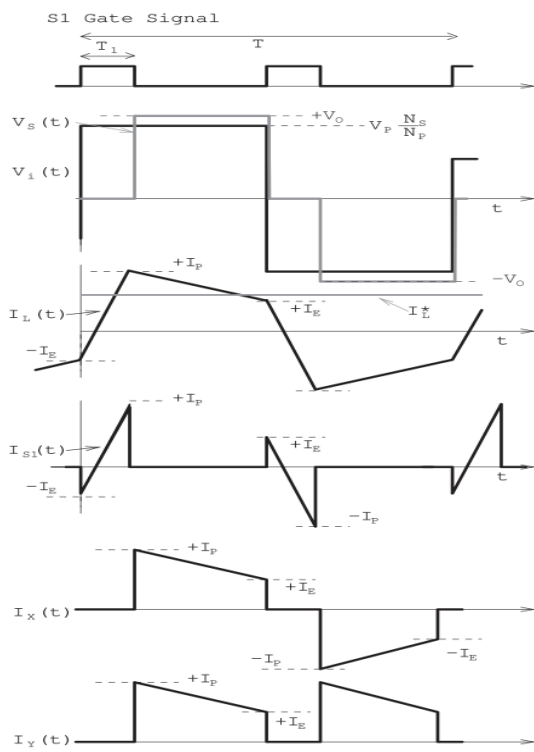
$$I_L^* = \left(T_1 \frac{T}{2} - T_1^2 \right) \frac{V_O}{T L_L}. \quad (3.12)$$

With $I^*L = G_M V_I$, then substituting in (12) and rearranging yields the equation

$$T_1 = \frac{T}{4} \left(1 - \sqrt{1 - \frac{16 G_M L_L V_I}{T V_O}} \right). \quad (3.13)$$



(a) Discontinuous conduction mode.



(b) Continuous conduction mode.

Fig. 2 Idealized waveforms. (a) Discontinuous conduction mode. (b) Continuous conduction mode.

Power Handling Capability

The converter's power capability is limited to being between 1.3 and a real number.3 if the GM requirement is taken into consideration. The square root of this must be positive and, as a result,

$$\frac{16G_{Mmax}L_L V_I}{TV_O} \leq 1$$

$$P_{max} = \frac{1}{2}G_{Mmax}V_{I_{max}}^2 \text{ of}$$

$$P_{max} \leq \frac{V_{AC} \frac{N_s}{N_p} V_O}{32\sqrt{2}f_s L_L} \quad (3.14)$$

This equation can be used as a basis for converter design as demonstrated by the prototype example in Section V. The maximum peak current in the leakage inductor during the CCM can be calculated as follows:

$$I_{Pmax} = \frac{V_O T}{8L_L} \quad (3.15)$$

And the transformer must be designed to handle this peak current without saturation.

4. POWER SUPPLY CONTROL

The control objective for the power supply is to provide a constant output voltage and unity input power factor. This requires measurement of the output voltage and adjustment of the input current through the GM factor

defined in Section III-A. However, calculating the time parameter T_1 in Section III-A and III-B also requires knowledge of the parameter L_L , the leakage

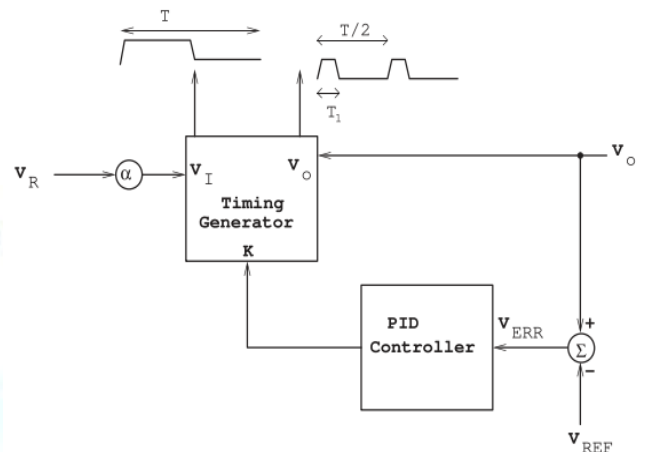


Fig. 3. Feedback control for the power supply.

Inductance, which may not be accurately known. Therefore a new control parameter K is defined as follows:

$$K = \frac{G_M L_L}{T} \quad (3.16)$$

And K is used for control rather than G_M . Substituting into (8) and (13) results in the required calculations for DCM as

$$T_1 = T \sqrt{K \left(\frac{V_O - V_I}{V_O} \right)} \quad (3.17)$$

And CCM as

$$T_1 = \frac{T}{4} \left(1 - \sqrt{1 - \frac{16KV_I}{V_O}} \right) \quad (3.18)$$

It can further be shown that the boundary condition of (4) can be written as follows:

$$V_O(1 - 4K) \geq V_I \quad (3.19)$$

Then, you can control the power supply in Fig. 3.4. In figure 3.4, the power supply voltage is compared to a reference voltage to produce voltage error figure this error voltage is used by a PID controller with a response slower than the input AC to control the output voltage.

Variable K is used twice to generate the inverter timing and once for secondary shorting in the sample period T . It has an input voltage of $2 V_p$ applied to it, and an output voltage of $V_R = 1 N_p$. If the result of (3.19) is true, the DCM is selected and T_1 is calculated. Otherwise, the CCM is used to calculate the time period T_1

5. RESULTS AND DISCUSSION

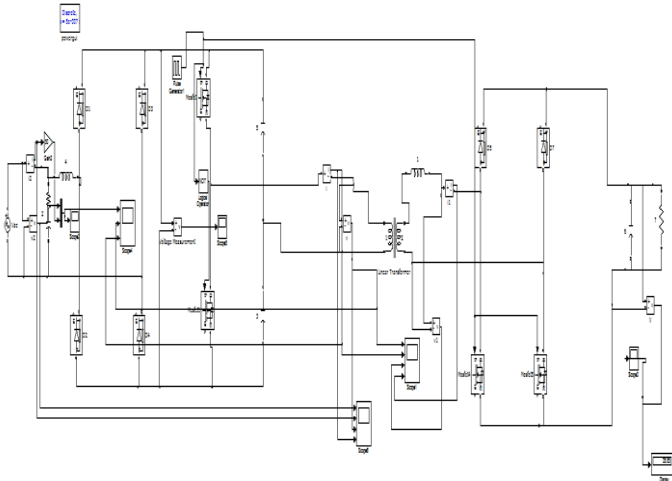


Fig 5.1 Simulink diagram of Proposed System Power Factor Corrected AC-DC power conversion

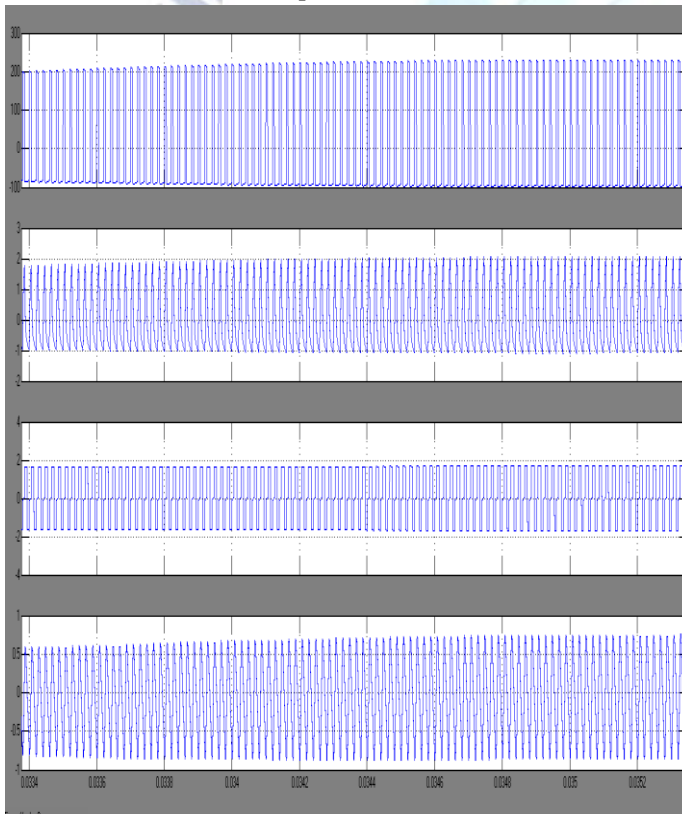


Fig. 5.2. Simulation waveforms at 300 W operation over a complete line cycle, input ac voltage (VAC) and current (IAC) and transformer primary voltage (VP) and current (IP)

Fig. 5.2 shows the line voltage and primary voltage measured as a waveform at full amplitude and time. The waveforms for the transformer voltages and currents are shown in Fig. 3 (DC) and Fig. 4 (CCM) for verification. The capacitors' finite values are easily seen in the primary voltage of Figure 5, which causes a decrease in voltage.

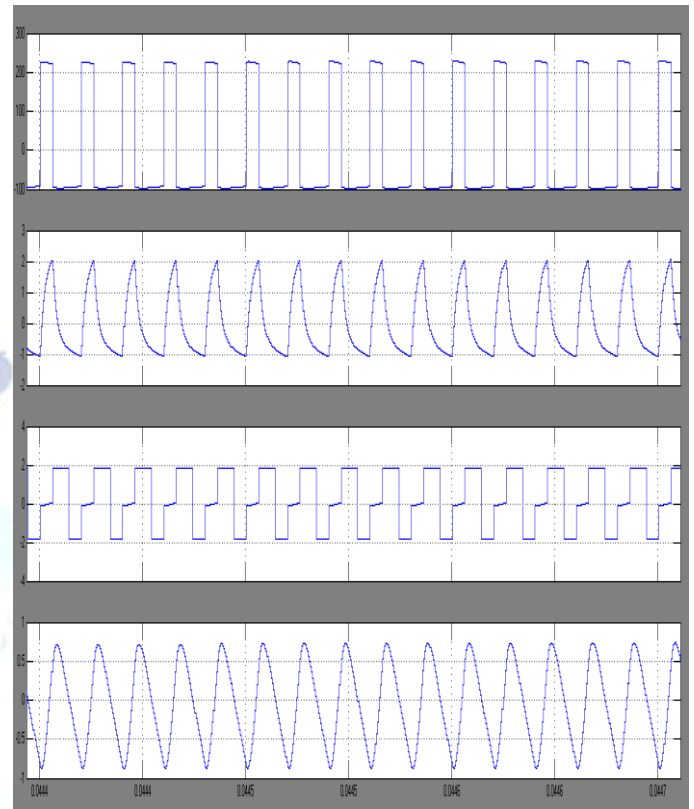


Fig. 5.3. Measured waveforms at 300 W operation, 1.5 ms from zero crossing and operating in DCM mode. Transformer primary voltage (VP) and current (IP) and secondary voltage (VS) and current (IS).

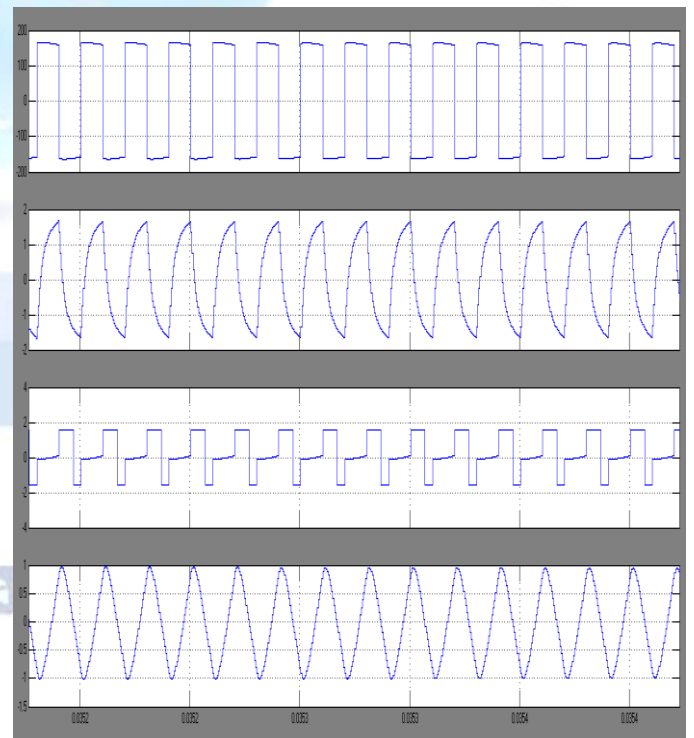


Fig. 5.4. Simulation waveforms at 300 W operation, 5 ms from zero crossing and operating in CCM mode. Transformer primary voltage (VP) and current (IP) and secondary voltage (VS) and current (IS).

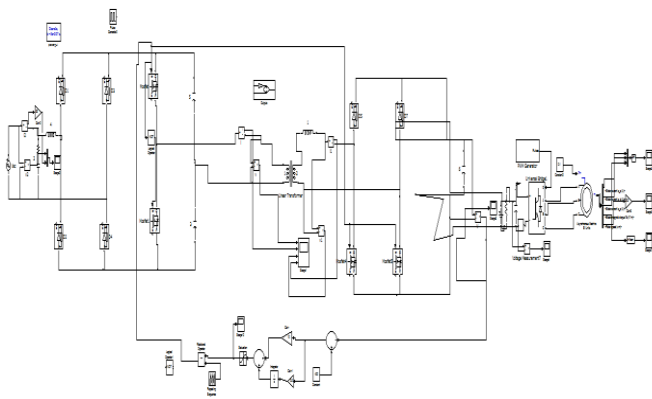


Fig 5.5 Simulink diagram of Proposed System Power Factor Corrected AC-DC power conversion with Induction Motor drive

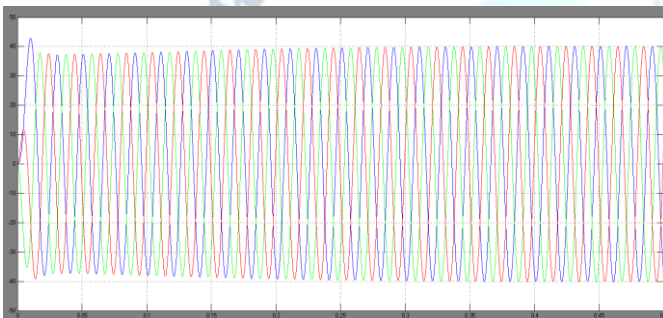


Fig 5.6 Simulation waveforms of Induction motor drive stator current characteristics

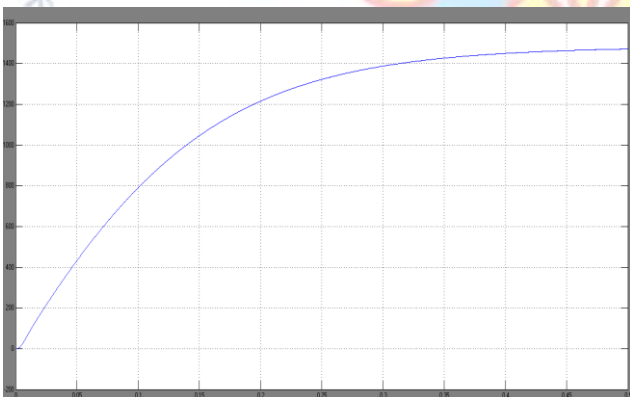


Fig 5.7 Simulation waveforms of Induction motor drive speed characteristics

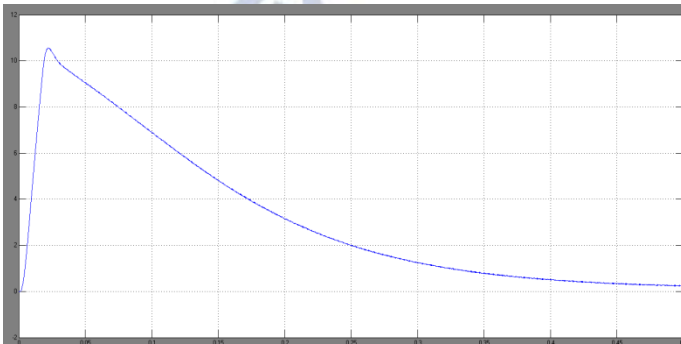


Fig 5.7 Simulation waveforms of Induction motor drive Torque characteristics

6. CONCLUSION

This paper presents an isolated ac/dc power supply by means of the transformer's active leakage. The proposed flyback PFC architecture allows for compact power levels that are less than the induction motor's demand. The control circuit is described in detail, and two-based on the principle of operation is developed for it. Measurements demonstrate the active power correction by power factor and THD. It is feasible to scale up the proposed circuit's capability to 500 W. A wider variety of methods can be employed, including universal input voltage operation, full bridge-input inverter designs, synchronous designs, and the like. provides an additional design space for the PFC design engineers. The induction motor was also verified.

REFERENCES

- [1] O. Garcia, J. A. Cobos, R. Prieto, P. Alou, and J. Uceda, "Single phase power factor correction: A survey," *IEEE Trans. Power Electron.*, vol. 18, no. 3, pp. 749–755, May 2003.
- [2] B. Singh, B. N. Singh, A. Chandra, K. Al-Haddad, A. Pandey, and D. P. Kothari, "A review of single-phase improved power quality AC-DC converters," *IEEE Trans. Ind. Electron.*, vol. 50, no. 5, pp. 962–981, Oct. 2003.
- [3] M. M. Jovanovic and Y. Jang, "State-of-the-art, single-phase, active power factor correction techniques for high-power applications—An overview," *IEEE Trans. Ind. Electron.*, vol. 52, no. 3, pp. 701–708, Jun. 2005.
- [4] N. Mohan, T. M. Undeland, and W. P. Robbins, *Power Electronics: Converters, Applications, and Design*. Hoboken, NJ, USA: Wiley, Oct. 2002.
- [5] T. Yan, J. Xu, F. Zhang, J. Sha, and Z. Dong, "Variable-on-time-controlled critical-conduction-mode flyback PFC converter," *IEEE Trans. Ind. Electron.*, vol. 61, no. 11, pp. 6091–6099, Nov. 2014.
- [6] D. G. Lamar, M. Arias, A. Rodriguez, A. Fernandez, M. M. Hernando, and J. Sebastian, "Design-oriented analysis and performance evaluation of a low-cost high-brightness LED driver based on flyback power factor corrector," *IEEE Trans. Ind. Electron.*, vol. 60, no. 7, pp. 2614–2626, Jul. 2013.
- [7] C. Zhao, J. Zhang, and X. Wu, "An improved variable on-time control strategy for a CRM flyback PFC converter," *IEEE Trans. Power Electron.*, vol. 32, no. 2, pp. 915–919, Feb. 2017.
- [8] J. W. Shin, S. J. Choi, and B. H. Cho, "High-efficiency bridgeless flyback rectifier with bidirectional switch and dual output windings," *IEEE Trans. Power Electron.*, vol. 29, no. 9, pp. 4752–4762, Sep. 2014.
- [9] C.-P. Tung and H. S.-H. Chung, "A flyback AC/DC converter using power semiconductor filter for input power factor correction," in *Proc. IEEE Appl. Power Electron. Conf. Expo.*, Long Beach, CA, USA, 2016, pp. 1807–1814.
- [10] L. Gu, W. Liang, M. Praglin, S. Chakraborty, and J. M. Rivas Davila, "A wide-input-range high-efficiency step-down power factor correction converter using variable frequency multiplier

technique," IEEE Trans. Power Electron., vol. 33, no. 11, pp. 9399–9411, Nov. 2018.

- [11] K. Mino et al., "Novel bridgeless PFC converters with low inrush current stress and high efficiency," in Proc. Int. Power Electron. Conf. – ECCEASIA, Sapporo, Japan, 2010, pp. 1733–1739.
- [12] M. Alam, W. Eberle, and N. Dohmeier, "An inrush limited, surge tolerant hybrid resonant bridgeless PWM AC-DC PFC converter," in Proc. IEEE Energy Convers. Congr. Expo., Pittsburgh, PA, USA, 2014, pp. 5647–5651.
- [13] A. H. Memon, K. Yao, Q. Chen, J. Guo, and W. Hu, "Variable-on-time control to achieve high input power factor for a CRM-integrated buck-flyback PFC converter," IEEE Trans. Power Electron., vol. 32, no. 7, pp. 5312–5322, Jul. 2017.
- [14] H. S. Athab, D. Dah-Chuan Lu, A. Yazdani, and B. Wu, "An efficient single-switch quasi-active PFC converter with continuous input current and low DC-bus voltage stress," IEEE Trans. Ind. Electron., vol. 61, no. 4, pp. 1735–1749, Apr. 2014.
- [15] S. W. Lee and H. L. Do, "A single-switch AC-DC LED driver based on a boost-flyback PFC converter with lossless snubber," IEEE Trans. Power Electron., vol. 32, no. 2, pp. 1375–1384, Feb. 2017.

